Available online at www.sciencedirect.com
SCIENCE DIRECT®
Catalysis Today 85 (2003) 225–233
CATALYSIS TODAY
www.elsevier.com/locate/cattod

Selective oxidation of alcohols using octahedral molecular sieves: influence of synthesis method and property–activity relations

Vinit D. Makwana [a], L. Javier Garces [b], Jia Liu [b], Jun Cai [a], Young-Chan Son [a], Steven L. Suib [a,b,c,*]

[a] *Department of Chemistry, U-3060, University of Connecticut, Storrs, CT 06269-3060, USA*
[b] *Institute of Material Sciences, U-3060, University of Connecticut, Storrs, CT 06269-3060, USA*
[c] *Department of Chemical Engineering, U-3060, University of Connecticut, Storrs, CT 06269-3060, USA*

Abstract

Manganese oxides having a tunnel structure (OMS-2) have been utilized as selective catalysts for alcohol oxidation. In this study manganese oxide catalysts were synthesized in different media and modified by exchanging the tunnel cation by H^+, using acid treatment or exchanging with NH_4^+ followed by thermolysis. Various alcohol oxidations were performed using these catalysts to ascertain the influence of synthesis method on their activity. A correlation is made between lattice oxygen instability and activity of the catalysts, which indicates involvement of the lattice oxygen in the mechanism. The exchange of the tunnel cation with the smaller H^+ ions leads to weakening of the Mn–O bond, as verified by temperature programmed desorption (TPD) results. Only the chemisorbed oxygen on the surface (O^-) and the lattice oxygen in the layers close to the surface is involved in the oxygen transfer during the reaction.

Keywords: Octahedral molecular sieves; Alcohol oxidation; Lattice oxygen

1. Introduction

Metal oxides have been employed as catalysts for a variety of organic transformations. Industrially, transition metal oxides are most widely used for reactions ranging from cracking in the petroleum sector to alkylation in the petrochemicals area. Some oxides like TiO_2 are important photocatalysts and find applications in pollution control measures while others like ZrO_2 are used as catalyst supports. The oxides of manganese and chromium have been conventionally used as stoichiometric oxidizing agents for carrying out alcohol oxidations. However, the large amounts of heavy metal waste, especially Cr(VI), generated by this methodology act as a major drawback for their use [1]. This necessitates the need for milder, catalytic oxidation processes utilizing dioxygen or H_2O_2 as the oxidant [2].

Son et al. [3] have recently demonstrated a selective, catalytic alcohol oxidation using a mesoporous, tunnel-structured manganese oxide, using dioxygen as the oxidant. Further work on this system [4] pointed towards a Mars-van Krevelen mechanism where the involvement of the lattice oxygen was implicated as a factor for its selectivity. Many investigators [5,6] have studied the mechanism of participation of lattice oxygen in such systems involving metal oxide catalysts. These studies were directed towards finding the nature of adsorbed oxygen species and their reactivity, and also that of lattice oxygen. This report aims to extend the application of these tunnel-structured

* Corresponding author. Fax: +1-860-486-2981.
E-mail address: suib@uconnvm.uconn.edu (S.L. Suib).

0920-5861/$ – see front matter © 2003 Elsevier B.V. All rights reserved.
doi:10.1016/S0920-5861(03)00390-0

manganese oxides to the difficult to oxidize alkyl alcohols using suitable modifications of the catalyst. A structure–activity correlation is also drawn, which sheds light on the nature of the lattice oxygen participating in the oxidation mechanism.

2. Experimental

2.1. Reagents

All reagents used in the current study were of analytical grade unless otherwise noted.

2.2. Catalyst synthesis

The catalysts used in the present study belong to a class of synthetic manganese oxide materials with a tunneled structure, called octahedral molecular sieves (OMS) [7,8]. The synthetic OMS catalyst has a one-dimensional tunnel structure formed by 2×2 edge shared MnO_6 octahedral chains, and is called OMS-2 (Fig. 1). The tunnels have dimensions of 4.6 Å × 4.6 Å, while the overall composition is $KMn_8O_{16}{\cdot}nH_2O$.

K-OMS-2 was prepared by a precipitation method [9]. A 0.4 M solution of potassium permanganate was added drop-wise with vigorous stirring to a mixture of a 1.75 M solution of manganese sulfate monohydrate and 6.8 ml of concentrated nitric acid. The resulting black precipitate was stirred and refluxed at 373 K for 24 h. The precipitate was filtered and washed with distilled, deionized water until neutral pH and then dried overnight at 393 K. The final powder obtained was named OMS-2-1a.

Thus prepared K-OMS-2 was ion-exchanged with H^+ to give H-K-OMS-2. OMS-2-1a was added to a 1 M solution of nitric acid and stirred at 333 K for 3 h. After filtering and a similar washing and drying procedure, the black powder obtained was denoted as OMS-2-1b. This treatment does not lead to a total exchange of K^+ by H^+. Another strategy employed towards this end was exchanging K^+ with NH_4^+ followed by thermolysis to reduce the NH_4^+ to H^+. OMS-2-1a was added to a 25 ml of 20% (w/v) solution of ammonium nitrate and stirred at room temperature for 3 h. The slurry was allowed to settle and the clear liquid phase was separated by decantation. A fresh 25 ml of the same 20% solution of ammonium nitrate was added and again stirred for 3 h at room temperature. The solution was filtered, washed and dried before calcining at 400 °C in air for 8 h. This treatment was enough to reduce all the NH_4^+ to H^+ as determined by analyzing the exhaust gases. This resulting catalyst was labeled OMS-2-1c.

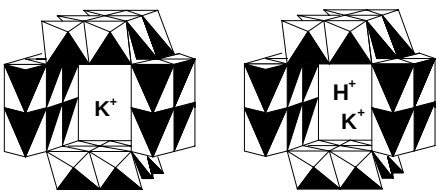

Fig. 1. Structure of OMS-2 catalysts.

Another method of synthesizing OMS-2 in neutral medium has been previously reported [10]. A sol was prepared by dissolving 0.01 mol of potassium nitrate and 0.0046 mol of manganese(II) nitrate in 50 ml of distilled, deionized water. A solution of glucose, which acts as a cross-linking agent, was added to this solution such that the molar ratio of salt to cross-linking agent was 1:2. The resulting clear solution was stirred for 10–30 min, followed by heating to evaporate all the water. A gel was formed at this point, which was heated in air at 180 °C for 2 h to give a dark black powder. This product was calcined from 300 to 800 °C in a stepwise ramp, with a 2 h hold time at each interval. The final product was characterized to be OMS-2 and is labeled as OMS-2-2a. This catalyst was modified by treatment with 1 M HNO_3 and ion-exchanged with NH_4^+ followed by calcination similarly as described for OMS-2-1a. These treatments yielded materials OMS-2-2b and OMS-2-2c, respectively.

OMS-2 has also been synthesized in basic medium [11]. According to this synthesis procedure, 0.038 mol of manganese(II) chloride tetrahydrate were dissolved in 50 ml of distilled, deionized water. A 6.25 M solution of sodium hydroxide was added drop-wise to this solution to precipitate out a birnessite precursor. After 6 h of stirring, the resulting birnessite was filtered, washed and ion-exchanged with a potassium chloride solution to form K-birnessite. The K-birnessite was filtered, washed, and dried before calcining at 200–800 °C in 200 °C intervals, with a hold time of

2 h at each interval. This calcination treatment yielded cryptomelane, which is denoted as OMS-2-3a. This catalyst was also modified by treatment with 1 M HNO_3 and ion-exchanged with NH_4^+ followed by thermolysis to yield materials labeled OMS-2-3b and OMS-2-3c, respectively. Thus we have synthesized cryptomelane in acidic, neutral, and basic medium and the effect of synthesis method on activity can be evaluated.

2.3. Surface area measurements

The surface area of each material was measured by the Brunauer–Emmett–Teller (BET) method on a Micromeritics ASAP 2010 instrument. The measurements were made using nitrogen as the adsorbent and with a multi-point method.

2.4. X-ray powder diffraction studies

The structure of all materials was verified by X-ray diffraction experiments. Data were collected using a Scintag 2000 PDS instrument with Cu Kα radiation with a beam voltage of 45 kV and a beam current of 40 mA. The structure was matched to standards and was found to be conserved even after the H^+ exchange treatments.

2.5. Chemical composition measurements

The morphology of the catalysts was studied by scanning electron micrographs taken on an AMRAY 1810 scanning electron microscope. The chemical compositions were determined by an energy dispersive X-ray (EDAX) analysis on a Philips PV 9800 EDAX spectrometer using a SuperQuant program. This analysis provides a measure of the amount of tunnel K^+ cations exchanged by H^+ in the modified catalysts.

2.6. Average oxidation state

The average oxidation state (AOS) of the manganese in the Mn^{2+}, Mn^{3+}, and Mn^{4+} containing OMS-2 catalyst was measured by potentiometric titrations [12]. The catalyst was dissolved in concentrated hydrochloric acid so as to convert all the manganese to Mn^{2+}, and titrated to a Mn^{3+} complex with sodium pyrophosphate versus potassium permanganate. This gave the total Mn content, based on which the AOS is determined by reducing the solid to Mn^{2+} by ferrous ammonium sulfate and back-titrating the excess Fe^{2+} with permanganate standard.

2.7. Temperature programmed desorption

Temperature programmed desorption with mass spectrometric (TPD–MS) analysis of exhaust gases was used to ascertain the thermal stability of the catalysts. About 30–40 mg of the catalyst was packed into a quartz tube and loaded into a tubular furnace controlled by an Omega temperature controller. The sample was purged with UHP He (Matheson) for 6–8 h at room temperature followed by heating the sample to 700 °C at 15 °C/min. The He carrier gas at the exhaust was fed to a MKS-UTI PPT quadrupole residual gas analyzer and evolution of water, oxygen and carbon dioxide was monitored.

2.8. Catalyst activity measurement

The catalyst activity was quantified by performing a series of alcohol oxidations. Typically, a semi-batch, slurry reactor was used in which 15 ml of toluene (J.T. Baker), 1 mmol of the substrate alcohol and 0.5 mmol of methyl benzoate (Aldrich), as the internal standard, were charged. Then, 0.5 equiv of the catalyst were added and a reflux condenser was attached. Air, as an oxygen source, was bubbled at a high flow rate of ∼200 ml/min through the reaction mixture which was vigorously stirred. These steps ensured that mass transfer effects were overcome and the reaction was performed in the kinetic regime. The reactor was placed in a constant temperature paraffin oil bath. The reaction was carried out under toluene reflux (383 K) for 4–20 h. The alcohol substrates used were benzyl alcohol, 2-butanol, and cyclohexanol.

Gas chromatography–mass spectrometry (GC–MS) methods were used for the identification and quantification of product mixtures. The GC–MS analyses were done on a HP 5890 Series II gas chromatograph coupled with a HP 5971 mass selective detector. The column used was a HP-1 (cross-linked methyl siloxane) with dimensions of 12.5 m × 0.2 mm × 0.33 μm film thickness.

3. Results

3.1. Surface area measurements

The surface areas of the synthesized OMS-2 materials are shown in Table 1. The areas varied by <5% after ion-exchange treatments. These OMS-2 materials are low surface area oxides. The synthesis in acidic medium results in the largest surface area ($\sim$65 $m^2\,g^{-1}$) material, while the materials synthesized in basic or neutral medium with a high temperature (HT) calcination step have much smaller surface areas ($\sim$15 $m^2\,g^{-1}$), as expected.

Table 1
Surface areas of synthesized catalysts

Catalyst	Surface area ($m^2\,g^{-1}$)
OMS-2-1a	62
OMS-2-2a	14
OMS-2-3a	13

3.2. Chemical composition

The scanning electron micrographs show a fibrous, needle-like morphology of OMS-2, which remains unchanged after tunnel cation substitution. A representative SEM micrograph showing these details can be seen in Fig. 2. From the EDAX analysis measurements and based on the amounts of K^+ cations remaining after each catalyst modification treatment, the percentage of K^+ exchanged by H^+ can be determined. These SEM–EDAX results are seen in Table 2. For the materials prepared in acidic and neutral medium, treatment with HNO_3 results in a $\sim$20% exchange and exchange with NH_4^+ followed by thermolysis improves upon this percentage. However, for the materials prepared in basic medium, the acid as well as

Table 2
Extent of H^+ exchange in synthesized catalysts

Catalyst	% K^+ exchanged by H^+
OMS-2-1a	0
OMS-2-1b	21
OMS-2-1c	51
OMS-2-2a	0
OMS-2-2b	17
OMS-2-2c	38
OMS-2-3a	0
OMS-2-3b	53
OMS-2-3c	55

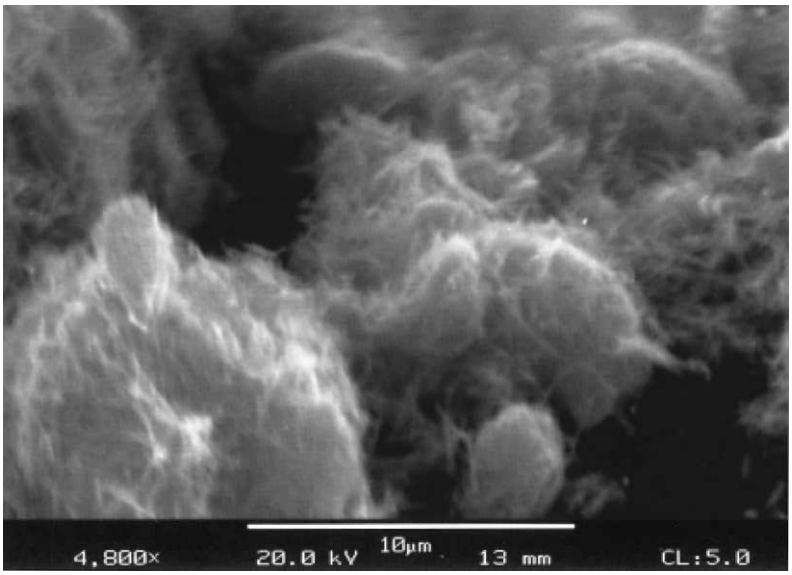

Fig. 2. SEM micrograph of OMS-2-1a.

Table 3
AOS of Mn in OMS-2 prepared by different methods

Catalyst	AOS
OMS-2-1a	3.81
OMS-2-2a	3.56
OMS-2-3a	3.67

NH_4^+ exchange protocol are equivalent and both result in a ∼50% exchange of K^+ by H^+. In all cases, the maximum extent of exchange was not greater than 55%.

3.3. Average oxidation state

The AOS gives an estimate of the electron environment around Mn centers. The AOSs of the as-synthesized OMS-2 materials varied from 3.56 to 3.81, as shown in Table 3. A material, OMS-2-1d, was obtained by exchanging OMS-2-1a with a higher strength of HNO_3. This was done in order to get a number of data points to understand the effect of H^+ exchange on AOS. Table 4 illustrates the trend of decreasing AOS with increasing extent of K^+ exchanged by H^+.

Table 4
Effect of K^+ exchanged by H^+ on AOS of Mn in OMS-2

Catalyst	AOS	% K^+ exchanged by H^+
OMS-2-1a	3.81	0
OMS-2-1b	3.75	21
OMS-2-1d	3.63	35
OMS-2-1c	3.55	51

3.4. Temperature programmed desorption

The effect of H^+ exchange on the structural stability of the catalyst is studied by TPD. Fig. 3 shows the evolution of oxygen from OMS-2-1a/1b and 1c as a function of temperature. This oxygen peak is the lattice oxygen liberated due to heating in a He atmosphere. The temperature at which the oxygen peak appears is the temperature at which the Mn–O bond is broken and is the thermal stability limit for that material. Yin et al. [13–15] have classified the oxygen peaks as low temperature (LT), medium temperature (MT), and HT peaks, based on their evolution temperature. The OMS-2-1b, which has 20% K^+ exchanged by H^+ shows very little change from the pure K-OMS-2. Since the *Y*-axis has arbitrary units,

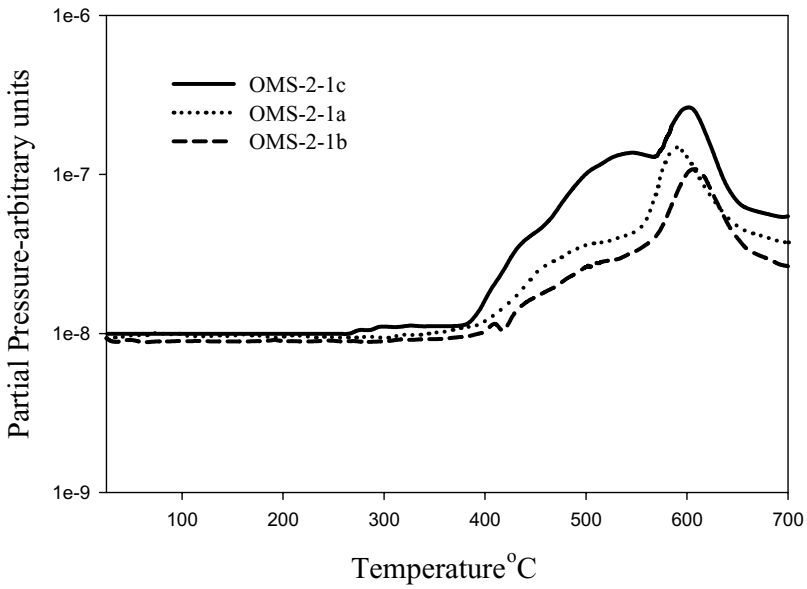

Fig. 3. TPD of OMS-2-1a/1b/1c in He.

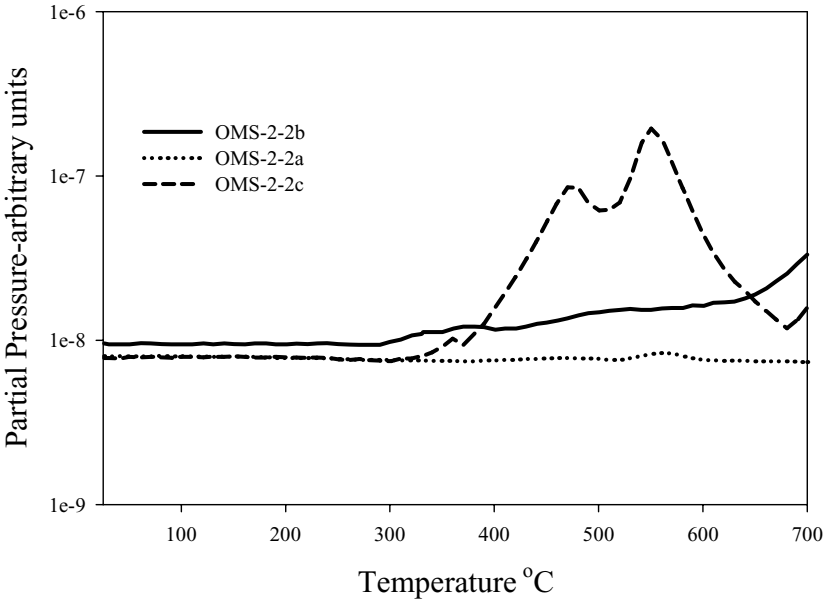

Fig. 4. TPD of OMS-2-2a/2b/2c in He.

the position of the O-evolution peaks and relative intensities, need to be analyzed. As the percentage of K^+ exchanged increases to 50% in OMS-2-1c, a significant change is seen in the intensities of LT and MT peaks.

The same results for the OMS-2-2a/2b and 2c series of materials are seen in Fig. 4. Since this is a material synthesized at HTs (800 °C), we see only the LT peak for OMS-2-2a before 700 °C. The HT synthesis makes the surface more "compact", energetically; resulting in most of the LT and MT species being already lost, or they are shifted to much higher temperatures, which are not reached in this experiment. For OMS-2-2b, the LT and MT peak are visible but weakly resolved, while the HT peak just starts to appear under 700 °C. As the H^+ percentage increases in OMS-2-2c, the MT peaks increase in intensity and are well differentiated. The peak positions are not affected drastically by the percentage of substitution of K^+ by H^+, but they do vary from the pure K-OMS-2 material. Fig. 5 shows the TPD data for the OMS-2-3a/3b and 3c materials. This material is obtained by calcination at 800 °C; hence we see a tiny LT peak for the unsubstituted K-OMS-2 and the beginning of the MT peak. The percentage of K^+ exchanged by H^+ is approximately the same for OMS-2-3b and 3c and their TPD profiles are also similar. The LT peak is relatively sharp and occurs almost 150 °C before the pure K-OMS-2 material. The MT peaks are weakly resolved and the HT peak is barely visible before 700 °C.

3.5. Catalyst activity results

The effect of different synthetic methods and different extents of tunnel cation substitution on the catalytic activity of these OMS-2 materials was studied by the conversion of alcohols to aldehydes or ketones. The results of these batch reactor studies are tabulated in Table 5. Benzyl alcohol being the most activated alcohol shows maximum conversion with each of the catalysts, while the secondary alkyl alcohols—2-butanol and cyclohexanol, show limited conversion. The reactions were carried out for 20 h, except for the oxidation of benzyl alcohol with the OMS-2-1 series of materials, which was carried out for 4 h. The materials showed 100% selectivity for benzaldehyde, 2-butanone, and cyclohexanone, respectively, and no over-oxidation to the carboxylic acid was observed. The OMS-2 materials prepared in acidic medium under water reflux have the highest

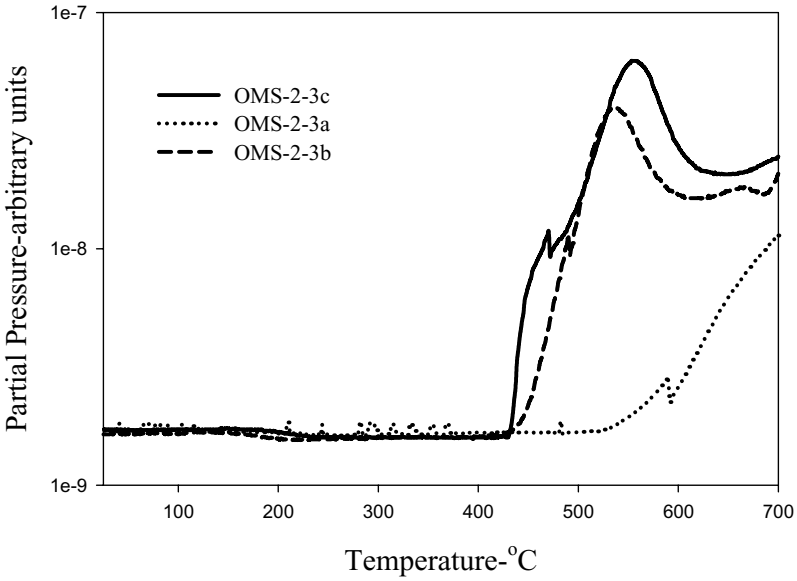

Fig. 5. TPD of OMS-2-3a/3b/3c in He.

surface areas and the highest activity for all three substrates. The other two catalysts synthesized at 800 °C show much less surface area and activity, with the material synthesized in neutral medium being more active than the material synthesized in basic medium.

Table 5
Reactivity of synthesized catalysts[a]

Catalyst	Surface area ($m^2\ g^{-1}$)	Conversion %[b]		
		2-Butanol	Cyclohexanol	Benzyl alcohol
OMS-2-1a	62[c]	37	28	90[d]
OMS-2-1b	62	41	41	95[d]
OMS-2-1c	62	41	60	95[d]
OMS-2-2a	14[c]	14	10	16
OMS-2-2b	14	16	14	42
OMS-2-2c	14	30	26	50
OMS-2-3a	13[c]	7	5	14
OMS-2-3b	13	12	15	35
OMS-2-3c	13	15	19	38

[a] Reactions in a slurry, batch reactor under toluene reflux for 20 h.

[b] Selectivity was 100% to 2-butanone, cyclohexanone and benzaldehyde.

[c] Change in surface areas of ion-exchanged materials (i.e. 1b, 1c, 2b, 2c, 3b, 3c) was <5%.

[d] Reaction carried out for 4 h.

4. Discussion

Tsuji and Abe [16] and Gehain et al. [17] have reported methods of progressive exchange of K^+ cations in cryptomelane (OMS-2) by H^+ to form cryptomelane type manganic acid (CMA). Although these methods lead to complete exchange of K^+ by H^+, they involve exchange with concentrated nitric acid for periods of up to 3 weeks, or reduction by hydrazine hydrate. The methods reported in this paper are much milder and quicker and are practical for up to 50% tunnel cation substitution with the tunnel structure being conserved. The thermal stability of OMS-2 materials modified by ion-exchange was ascertained by doing TPD. In each of the materials synthesized, irrespective of the pH of the synthesis medium, the TPD results show a larger oxygen evolution peak after exchange of the tunnel cation by the smaller H^+. Based on quantitative studies of these oxygen evolution peaks, Yin et al. have assigned the tiny LT peaks to a small amount of chemisorbed oxygen on the catalyst surface. The MT peak corresponds to structural oxygen from the lattice layers close to the surface. The loss of oxygen from these layers results in lattice vacancies, but the number of vacancies is small enough that the tunnel structure is conserved. The large HT oxygen peak

again corresponds to structural oxygen, but because of its magnitude, the loss of this oxygen leads to a breakdown of the structure, accompanied with a stepwise reduction of the manganese oxide to Mn_2O_3 and finally to MnO. As illustrated by the TPD results, a major effect of the tunnel cation substitution is on the LT and MT oxygen peaks. The HT peaks are not seen for the materials synthesized at HTs. Since the amount of chemisorbed oxygen is much smaller compared to the oxygen evolved in the MT peak, the lattice oxygen near the surface undergoes a major change. Iwamoto et al. [18] have studied oxides of Fe, Co, Ni, Cu, Al, Si, Ti and others by TPD techniques and shown the presence of three desorbed oxygen peaks as a typical result, with similar peak assignments.

All the synthesized and modified materials were tested for activity by using them as catalysts to perform alcohol oxidations (Table 5). The substrates chosen were a benzylic alcohol, a secondary linear alcohol (2-butanol) and a secondary cyclic alcohol (cyclohexanol). The rate-determining step [4] is the formation of a carbocation, which is stabilized by resonance delocalization in the case of benzylic alcohols; hence benzyl alcohols show the maximum conversion with all materials. Secondly, as the catalysts are modified by exchanging the tunnel K^+ with H^+, there is a direct correlation between percentage of K^+ exchanged and its activity. This, combined with the TPD results, corroborate the involvement of lattice oxygen in the reaction mechanism.

Post et al. [19,20] have performed X-ray diffraction studies on cryptomelane and its alkali cation-exchanged forms. According to these, cryptomelane has a tetragonal geometry, but is known to distort to a monoclinic geometry when the ratio of the lattice Mn ionic radius over the tunnel cationic radius exceeds a value of 0.48. Based on the calculated lattice parameters, this transition is due to torsion of the tunnels resulting in elongation of the '*a*' parameter. Since the ionic radius of H^+ is much smaller than that of K^+, this condition is satisfied, and the cryptomelane lattice is strained, which in turn strains the Mn–O bonds. As a result of this strain, lattice oxygen is evolved much more readily in the ion-exchanged material than the pure K-OMS-2, which is shown in the TPD results. From a previous report [4], this system acts via a Mars-van Krevelen mechanism, which involves lattice oxygen. As lattice oxygen instability increases with increasing ion-exchange, the activity of the catalyst also increases. The major difference is in the LT and MT peaks in the TPD results. Therefore, lattice oxygen in the layers near the surface plays an important role in this oxidation. Another effect of the tetragonal to monoclinic transition is the increase in the number of Mn^{3+} sites, due to oxygen loss as a result of strained Mn–O bonds. This is also favored because of the larger ionic radius of Mn^{3+} compared to Mn^{4+}, which fits better in a monoclinic environment. As the number of Mn^{3+} sites increases due to tunnel cation-exchange, the AOS of Mn in the material would decrease, as is borne out by the AOS results in Table 3.

5. Conclusions

Cryptomelane type manganese oxides (OMS-2) have been synthesized in different media and modified by exchanging tunnel cations with H^+. This exchange is carried out by acid treatment or exchange with NH_4^+, followed by thermolysis. These materials were used as catalysts for performing alcohol oxidations. The material with the highest surface area, which was synthesized in acidic medium at LT, shows the maximum activity. The activity is maximum for benzylic alcohols, while selectivity of 100% is maintained for all the alcohol substrates tested. The thermal stability of these catalysts was probed by TPD, and was found to decrease with increasing percentage of tunnel cation-exchange. The reaction over OMS-2 catalysts occurs by a Mars-van Krevelen mechanism, involving exchange of the lattice oxygen. Since the TPD results show a major effect on the lattice oxygen in layers close to the surface, which is directly correlated to the increased activity towards alcohol oxidation, it is proven that only lattice oxygen close to the surface participates in the reaction. Loss of this oxygen creates nucleophilic vacancies in the lattice while maintaining the tunnel structure, which are replenished by gas phase oxygen. This explains the catalytic and selective nature of OMS-2 towards alcohol oxidation.

Acknowledgements

We acknowledge support by the Geosciences and Biosciences Division, Office of Basic Energy

Sciences, Office of Science, US Department of Energy. We would also like to thank Dr. Francis Galasso for many helpful discussions.

References

[1] S.V. Ley, A. Madin, in: B.M. Trost, I. Fleming, S.V. Ley (Eds.), Comprehensive Organic Synthesis, vol. 7, Pergamon Press, Oxford, 1991, p. 251.
[2] G.J. Brink, I.W.C.E. Arends, R.A. Sheldon, Science 287 (2000) 1636.
[3] Y.-C. Son, V.D. Makwana, A.R. Howell, S.L. Suib, Angew. Chem. Int. Ed. Engl. 40 (22) (2001) 4280;
Y.-C. Son, V.D. Makwana, A.R. Howell, S.L. Suib, Angew. Chem. 40 (113) (2001) 4410.
[4] V.D. Makwana, Y.-C. Son, A.R. Howell, S.L. Suib, J. Catal. 210 (2002) 46.
[5] H.H. Kung, Studies in Surface Science and Catalysis 45, Transition Metal Oxides: Surface Chemistry and Catalysis, Elsevier, Amsterdam, 1989.
[6] M. Che, G.C. Bond, Studies in Surface Science and Catalysis 21, Adsorption and Catalysis on Oxide Surfaces, Elsevier, Amsterdam, 1985.
[7] Y.F. Shen, R.P. Zerger, R.N. DeGuzman, S.L. Suib, L. McCurdy, D. Potter, C.L. O'Young, J. Chem. Soc., Chem. Commun. (1992) 1213.
[8] Y.F. Shen, R.P. Zerger, R.N. DeGuzman, S.L. Suib, L. McCurdy, D. Potter, C.L. O'Young, Science 260 (1993) 511.
[9] R.N. DeGuzman, Y.F. Shen, S.L. Suib, B.R. Shaw, C.L. O'Young, Chem. Mater. 5 (1993) 1395.
[10] J. Liu, J. Cai, X.F. Shen, S.L. Suib, M. Aindow, Mater. Res. Soc. Symp. Proc. 755 (2003) DD6. 24. 1.
[11] J. Cai, J. Liu, W.S. Willis, S.L. Suib, Chem. Mater. 13 (2001) 2413.
[12] D. Glover, B. Schumm Jr., A. Kozowa, Handbook of Manganese Dioxides Battery Grade, International Battery Materials Association, Cleveland, 1989.
[13] Y.G. Yin, W.Q. Xu, R.N. DeGuzman, S.L. Suib, C.L. O'Young, Inorg. Chem. 33 (1994) 4384.
[14] Y.G. Yin, W.Q. Xu, Y.F. Shen, S.L. Suib, C.L. O'Young, Chem. Mater. 6 (1994) 1803.
[15] Y.G. Yin, W.Q. Xu, S.L. Suib, C.L. O'Young, Inorg. Chem. 34 (1995) 4187.
[16] M. Tsuji, M. Abe, Solvent Extr. Ion Exch. 2 (1984) 253.
[17] E.D. Gehain, P.C. Picquet, C.J. Spears, F.L. Tye, Prog. Batteries Battery Mater. 13 (1994) 62.
[18] M. Iwamoto, Y. Yoda, N. Yamazoe, T. Seiyama, J. Phys. Chem. 82 (24) (1978) 2564.
[19] J.E. Post, R.B. vonDreele, P.R. Buseck, Acta Cryst. B 38 (1982) 1056.
[20] M. Tsuji, S. Komarneni, J. Mater. Res. 8 (12) (1993) 3145.